Enhancing the Interpretation of I*n Vitro* Bioaccessibility Data by using Computer Controlled Scanning Electron Microscopy (CCSEM) at the Individual Particle Level

Jane A. Entwistle[a], Andrew Hunt[b]*, Ndokiari Boisa[a1] and John R. Dean[c],

[a] Department of Geography, Northumbria University, Newcastle-upon-Tyne, NE1 8ST, U.K. (jane.entwistle@northumbria.ac.uk)

[b] Department of Earth and Environmental Sciences, University of Texas at Arlington, Arlington, TX 76019, U.S.A. (hunt@uta.edu)

[c] Department of Applied Sciences, Northumbria University, Newcastle-upon-Tyne, NE1 8ST, U.K. (john.dean@northumbria.ac.uk)

[1] (Present address: Department of Chemistry, Rivers State University of Science and Technology, Nigeria)

*Corresponding Author: Andrew Hunt, Ph.D. hunt@uta.edu
Tel: 817 272 0437

ABSTRACT

The adverse health effects resulting from exposure to contaminated soil on internally displaced populations in Mitrovica, Kosovo can be determined by how the potentially harmful elements are bound in the soils. Certainly this was the case for Pb, present at concentrations ranging from 624 to 46,900 mg/kg, and at bioaccessibilities ranging <5% to nearly 90%. To assess why the soil Pb might differ so markedly in terms of its bioaccessibility, computer controlled scanning electron microscopy (CCSEM) was employed to determine how the Pb was associated with other elements at the individual particle (IP) level in soils from the area. It was found that the Pb-bearing particle types were, for the most part, different in each sample. We consider these differences as the main control on Pb bioaccessibility in these soils. Pb solubility at the IP level was evaluated by examining Pb-particles from these soils in the electron microscope before and after successive immersions in a simulated gastric fluid. This analysis (differential IP analysis) confirmed the CCSEM characterization that Pb associated with other higher atomic number elements (Fe, Zn, Cu and Ni) was less soluble than when it was present as isolated phases (e.g., as carbonate) or when it was bound with lower atomic number elements (Na, Al, Si, K, Ca). The heterogeneity in solubility and composition of the Pb-particles suggested that the Pb originated from a range of different anthropogenic activities. The nature of these different anthropogenic activities created the wide differences in Pb-bioaccessibilty by producing Pb bound in many different forms in the soil particles. This type of Pb-particle characterization highlights the role CCSEM analysis, and IP acid extraction, can play in providing supporting evidence alongside

bioaccessibility data for applications in human health risk assessment and management of contaminated soil.

KEYWORDS: Soil; Metals; SEM; Pb; Bioaccessibilty;

CAPSULE

CCSEM-EDS was used to collect particle composition data to better refine risk-based assessments and site management strategies.

INTRODUCTION

Potentially harmful elements (PHE) fall within the USFDA (2016) definition of any chemical or chemical compound that causes or has the potential to cause direct or indirect harm. The geochemistry of PHE controls their partitioning in the environment, their mobility, transport and ultimately their fate. In the case of PHE in soils, a variety of sequential chemical extraction procedures have been used to determine PHE partitioning in bulk soil samples in order to assess potential mobility. Such methods selectively remove specific constituents from unconsolidated samples (such as soils) for the purpose of determining the fractions to which the PHEs of interest are bound (Young et al., 2005). Sequential extraction methods can be extremely complicated (see, e.g., Bacon and Davidson, 2008), and may fail to address questions pertinent to human health risk assessment. Not all forms of ingested PHEs are solubilized in the gastrointestinal (GI) tract with obvious human health consequences. Due to the potential for adverse health outcomes associated with the ingestion (inadvertent or otherwise) of contaminated soil, considerable attention has focused on measuring the bioavailability, or more specifically the *in vitro* bioaccessibility, of PHEs (e.g. Cai et al., 2016; Li et al., 2014; Lorenzi et al., 2012; Okorie et al., 2011; Smith et al., 2011). Oral bioaccessibility protocols seek to model the extraction of PHEs during the passage of material through the human GI system and numerous studies have reported that the mineralogical form/solid phase partitioning of the contaminant has a large influence on its bioaccessibility (Cox et al., 2013; Palumbo-Roe et al., 2013; Pelfrene et al., 2012; Reis et al., 2014; Walraven et al., 2015; Wragg and Cave, 2012). Furthermore, a number of studies have indicated a complex range of percentage bioaccessibility data across contaminated sites

(e.g. Farmer et al., 2011; Okorie et al., 2011; Roussel et al., 2010). This poses questions for regulators and risk managers when assessing contaminated land in terms of the reliability of bioaccessibility data and how to best interpret, and apply, such data. Interpretation of *in vitro* bioaccessibility data from the analysis of bulk soil samples can be enhanced by an examination of how element constituents are bound at the individual particle (IP) level. Electron microscopy based methods that can capture the variety of element associations in particles in soils by analyzing thousands of particles will provide insights into the solid phase speciation that controls bulk *in vitro* bioaccessibility.

To test this hypothesis, here we report the results of an investigation into contaminated soils from city of Mitrovica, which is located in the Republic of Kosovo. Since historic times this area has been associated with mining, smelting and processing metal ores. Mitrovica is a small city (approximately 70,000 inhabitants) located in the District of Mitrovica, in northern Kosovo. Prior to the Kosovan War of 1998-1999, when various industrial enterprises stopped, several diverse metal-production operations were active. Metal ores were smelted at Zvecan, north of Mitrovica (Figure 1), with waste stored in the Zharkov Potok tailings pond and smelter slag disposed of at Gornje Polje waste dumps (also on the northern boundary of Mitrovica). In addition, industrial residues from a former chemical plant (located in south east Mitrovica) where Zn electrolysis, and Pb battery manufacture took place, are present over approximately 30 hectares of land on the banks of the Sitnica River that runs through Mitrovica (Figure 1)

Population exposure to PHE contaminated environmental media is of potential concern in this region. Previous work has demonstrated the potential public health problems associated with the intake of soil-bound PHEs present at various locations in this area (Boisa et al., 2013). Physiologically-based *in vitro* analyses (Boisa et al., 2013, 2014) showed that metal bioaccessibility in exposure media from the area was highly variable, and potentially could reach dangerously high levels of availability. This was clearly an issue during the Kosovan War, when the displacement of predominantly Roma and Ashkali populations from the Roma Mahalla neighborhood in south Mitrovica led to resettlement in locations that had not only high soil PHE levels, but also high PHE bioaccessibility levels. Relocation to the Osterode internally displaced peoples (IDP) camp (a former French barracks) and the Cesmin Lug IDP camp, both of which are within 300 m of the Gorne Polje tailings dump, and immediately downwind of the Zvecan smelter (Figure 1), provided an ideal opportunity for a public health calamity. Conceived originally as a temporary relocation, the camps were home for internally displaced families for almost 10 years. Elevated soil Pb levels here are of obvious concern given the adverse systemic health effects of Pb, and according to the Centers for Disease Control and Prevention no safe blood lead level (the biomarker for exposure) in children has been identified. Evidence for behavioural and cognition deficits resulting from low level Pb exposure is mounting (Budtz-Jørgensen et al., 2012; Chandramouli et al., 2009; Grandjean, 2010; Jakubowski, 2011; Lanphear, et al., 2005). A number of studies have also identified an association between early lead exposure and increased incidence of attention deficit hyperactivity disorder (ADHD) (Aguiar et al., 2010; Nigg et al., 2010), and other behavioral problems (Chen et al., 2007; Roy et al., 2009).

As part of this investigation into contaminated soils from Mitrovica, samples from the smelter waste site (from Gornje Polje), the tailing site (from Zharkov Potok), and topsoil samples (1-10 cm depth) from Bosniak Mahalla, Roma Mahalla and the ~~internally displaced peoples~~ IDP camp at Cesmin Lug were analysed (Figure 1). Investigation of the PHE associations (with a particular focus on Pb) at the IP level, proceeded in two stages using electron microscopy based methods. In the first, the objective was to determine whether the Pb-bearing particles differed significantly between sampling locations. The second objective was to assess how bioaccessible the particle bound Pb was at each location. To accomplish the first objective, computer controlled scanning electron microscopy (CCSEM), that combines scanning electron microscopy with energy dispersive X-ray spectroscopy (EDS) and automated image analysis software was used to collect IP composition data on a statistically significant numbers of particles from each sample. This analytical technique has been widely used to characterize particulate matter in a range of environmental media. For example, this approach has been used to evaluate long range transport of desert dusts (Coz, 2009; Reid et al., 2003), particle movement in urbanized desert areas (Wagner and Cassucio, 2014), the nature urban aerosols (Ault et al., 2012; Kumar et al., 2012; Lagudu et al., 2011; Moffet et al., 2008;), the content of indoor aerosols (Conner et al., 2001); and the metal-bearing particle content of soils (Johnson and Hunt, 1991; Kennedy et al., 2002). As CCSEM-EDS facilitates source identification it has the potential to support targeted interventions, or targeted remediation. The second objective was attained through a process of chemical extraction at the IP level. Lead particle solubility was investigated by Differential IP Analysis (DIPA). DIPA initially involved, in the first instance, the collection of IP information (elemental and morphological) in the SEM from particles as originally sampled. Then, upon

removal from the SEM the particles of interest were immersed *in situ* on the SEM mount in a simulated gastric fluid for a specified time. After returning the sample to the SEM particles previously analysed were relocated and analysed a second time to determine what differential changes may have occurred. DIPA has been used successfully in previous studies to gather information on the extent to which the different individual particles, or particle components, are more, or less, soluble than others (see e.g., Donner et al., 2012; Hunt and Johnson, 1996, 2010).

Lead-isotope ratio data for each sample was also collected to provide potentially supportive evidence for Pb-source separation. It has been shown that sources of Pb-contamination can, under certain circumstances, be identified based on differences in Pb-isotope ratios (e.g., Duzgoren-Aydin and Weiss, 2008; Gulson, 2008; Rabinowitz 1995). The stable Pb-isotope content of Pb-ores differ from each other (largely as a function of the age of the ore deposit), so if different sources of Pb are isotopically different (originating from different ores), and the contributing sources are limited in number, Pb-isotope source differentiation is possible.

MATERIALS & METHODS

Sampling

Surface samples from sites across the Mitrovica area were collected from 0 to 10 cm depth using a stainless steel trowel and then bagged, followed by air-drying, disaggregation and sieving to obtain the < 2 mm fraction. All soil samples were collected from communal residential or public recreational spaces within the study area. Five surface samples, representing each of the different sample locations in Mitrovica, were the subject of the detailed CCSEM-EDX investigation documented here. These samples were: a top soil from Bosniak Mahalla (BM5), a top soil from Roma Mahalla (RM45), IDP camp top soils (RM71, and RM72), tailings material from Zarkov Potok (RM66) and smelter waste from Gornje Polje (RM77).

Total concentration and oral bioaccessibility

Pseudo-total Pb (herein referred to as total) was determined by aqua regia digestion in a microwave oven (0.5 g sub-sample, HCl : HNO_3 in the ratio 3:1 v/v). The gastric-phase *in vitro* oral bioaccessibility was determined using the Unified Bioaccessibility method or UBM, after Wragg et al., 2009), modified for a 0.3 g sub-sample. These analyses were undertaken on a sieved <250 µm fraction. For each digestion (totals and gastric-phase), reagent blanks were also prepared and the filtrate obtained from the digestion was refrigerated (< 4°C) prior to analysis by ICP-MS (X Series II, Thermo Electron Corporation, Cheshire, UK). All chemicals used were certified analytical

grade and ultra-pure water of conductivity 18.2MΩ-cm was produced by a direct Q™ millipore system (Molsheim, France). The percentage bioaccessiblility was calculated as follows:

$$\% \text{ Bioaccessibility} = (C_{bio} / C_{total}) \times 100$$

Where C_{bio} is the concentration of Pb released from the soil (mg/kg) in the gastric phase extraction and C_{total} is the pseudo-total (aqua regia soluble) Pb concentration in the soil. Further details on the reference materials utilized and additional QC procedures are detailed in Boisa et al. (2013).

Computer Controlled Scanning Electron Microscopy (CCSEM)

The basics of the automated microscopy-based methodology used here, have been described previously by Hunt et al. (1992). In that study, the technique was employed to characterize particulate Pb derived from various types of source. Here the focus was exclusively on surface soils that were sieved through a < 64 µm nylon mesh. Finely divided material from this size fraction was prepared for CCSEM-EDS analysis in the following stages: (i) A subsample of material was placed in a 50 mL test tube containing distilled water to which a small amount (< 1 ml) of surfactant was added, this was then ultrasonically agitated for 5 minutes. (ii) An aliquot of the soil in water suspension was filtered, from a chimney reservoir, onto a 25 mm diameter 0.4 µm pore size polycarbonate membrane filter. (iii) Several filters were prepared for each sample so an optimal filter loading could be selected; a filter loading with a separation between particles of at least one particle diameter was considered optimal, however a filter with an even lighter loading was preferred. (iii) Each filter was attached to an SEM mount with an intervening layer of adhesive carbon paint, before it was submitted for analysis.

CCSEM analysis was performed on an ASPEX/FEI (now Thermo Fisher Scientific, Waltham, MA, USA) scanning electron microscope (SEM). The SEM was operated in variable pressure mode and specimen images were obtained from backscatter electron (BE) collection. Specimen composition information was determined by EDS using an ASPEX/FEI OmegaMax™ silicon drift detector with an ultra-thin window (permitting light element detection). The SEM standard operating conditions were: an accelerating voltage of 25 keV, a beam current of 1.0 nA, and a working distance of approximately 16 mm. The resident SEM automated feature analysis (AFA) software employed a BE signal (binary) threshold to separate the particles on the filter from the substrate. The binary threshold for AFA was set so that all features (particles) with an average atomic number greater than carbon were above the threshold. In automated feature search mode particles were detected based on the threshold. Upon feature detection, recording the element content of each feature detected involved the capture of X-ray data as the primary electron beam rastered in chords over the feature. The dwell time (the time the primary beam rastered over the particle) was set at a minimum of 10 seconds or the acquisition of 10,000 X-ray counts. For each feature an X-ray spectrum was collected and stored. Recognition of the elements in the feature X-ray spectrum used the AFA software vector editor. A vector being a pre-calculated data set performing quantitative analysis on unknown spectra. The type of vector calculated here (filter-fit) required reference spectra for individual elements; these were collected with the machine specific X-ray detector. The filter-fit technique assumes that the unknown feature spectrum can be represented as a weighted sum of the reference spectra. This weighted sum includes a constant called the k-ratio which is closely related to the weight

214 percentage. The elements of interest selected here for which percentage data was generated
215 were: Na, Mg, Al, Si, P, S, Cl, K, Ca, Ti, Cr, Mn, Fe, Ni, Cu, Zn, As, Sb, and Pb. In addition to element
216 concentration data, for each particle its size (e.g., minimum, maximum, and average diameter),
217 projected area, and aspect ratio were measured. This was stored in a database of > 4,500 features
218 that were analyzed for sample analysis.
219
220 The data interpretation phase focused on identifying homogenous groups of particle
221 types in the data sets obtained from each sample. A supervised divisive hierarchical cluster
222 analysis was used for this purpose. The existence of similarities in element concentration ranges
223 among the individual particles was the primary defining characteristic for a homogenous group.
224 The cluster analysis reached a stopping point where further division of a group was not necessary,
225 or when a new group would contain less than 1% of the total number of particles in the data set.
226 Based on the composition of the particles in each group, a set of rules was defined to classify
227 particles belonging to that group. In this rule set, each particle group (a particle class) was
228 ordered in a linear (classification) scheme to enable class attribution of the CCSEM data from
229 other samples. The rules that described a class were generally inclusionary and were delineated
230 by the percentage concentration ranges for the main elements identified in the particles in each
231 homogenous group. Classification of the particles in each of the samples was accomplished by
232 linearly sorting the CCSEM element data for each particle through the scheme.
233
234 **Differential Individual Particle Analysis (DIPA)**

A dry fraction of each sample was passed through a 64 um nylon mesh suspended above a 5cm x 5cm square of double sided adhesive carbon tape that was then subject to examination in the SEM. In early tests, double sided adhesive carbon tape was found to be preferable to other substrates (such as polycarbonate membrane filters) as deposited particles remained in place on the adhesive tape after any liquid immersion unlike particles deposited on a membrane filter. Analyst guided Pb-particle detection in the SEM was accomplished using high backscatter electron imaging. Lead-particle positions, once identified, were recorded using multiple saved images of the locational SEM fields of view (FOV). DIPA involved repeated exposure of Pb-particles of interest to a simulated gastric fluid (SGF) comprised of 0.4 M glycine, adjusted to pH 1.5 using concentrated HCl, at 37°C (USEPA, 2007). After initial SEM imaging, the particles were immersed in a droplet of SGF (applied by pipette onto the particles on the adhesive carbon tape) for repeated periods of 30 minutes up to a total of 2 hours. During these immersion intervals the sample was placed in a convection oven with the temperature set at 37°C. This process was intended to simulate the time over which ingested material resides in the stomach before transfer to the small intestine. At the end of the prescribed immersion period, the SGF was removed by pipette and replaced (again by pipette) with distilled water. This water was in turn removed and discarded and another quantity of water was immediately pipetted again onto the sample. This "washing" by dilution was repeated several times to remove as much SGF as possible from the sample and therefore stop the extraction. After each 30 minute SGF exposure, the sample was returned to the SEM and the FOVs of interest were relocated to allow the target Pb-particles to be imaged once more. This enabled any changes either physical and/or chemical changes that had occurred during SGF immersion to be recorded. This *in-situ* procedure has the

advantage of allowing the same particle to be re-examined after multiple exposures to assess potential dissolution rates over time.

Lead Isotope Determinations

Pb-isotopic ratios were determined for the < 64 μm size fraction of each sample. Pb-isotopes were measured using a VG Sector Ionization Mass Spectrometer (London, UK). The silica-gel technique was used and the filament temperature during measurements was monitored continuously and raw ratios measured at 1150 ^{o}C, 1200 ^{o}C, and 1250 ^{o}C. The reported Pb-isotopic data were corrected for mass fractionation of 0.12 $\pm$ 0.03% per a.m.u. based on replicate analyses of NBS-981 (common lead standard) equal atom Pb standard measured in the same manner. Estimated errors are less than 0.05% per mass unit. Values for procedural blanks were <400 pg for Sr, and <200 pg for both Nd and Pb.

RESULTS

Total concentration and oral bioaccessibility

The samples investigated had total Pb levels ranging from 624 – 46,900 mg/kg, and *in vitro* oral Pb bioaccessibilities of between 3.3 and 89% (Table 1).

The IDP camp topsoils have two very different bioaccessibilites, whilst Bosniak Mahalla is associated with a lower bioaccessibility than the Roma Mahalla topsoil. Both of the metalliferous wastes are associated with very low bioaccessibilities.

Computer Controlled Scanning Electron Microscopy (CCSEM)

A classification scheme containing classes for metal and non-metal particles was developed from the clustering exercise using a training set of data from one of the samples analyzed (BM5; selected as high pseudo-total Pb and moderate % bioaccessibility). The classes were subsequently refined by sifting the data from the other samples through the scheme. A total of 36 classes were originally developed, but for convenience a second scheme was subsequently formulated for only the Pb-bearing particles. Most classes were operationally defined, but some were obviously related to the mineral content of the soil. For example, the class containing particles with Si content >99%, was defined as "Si-only" but clearly represented a class for quartz. Similarly, the "Fe-only" class was a class for Fe-oxides, and the "Ca-only" class was for Ca-carbonate. Mixed element particles were also of specific "mineral types", namely: MgCa (class rule Mg+Ca>90%) defined dolomite, FeS (class rule Fe+S>95% and S>5%) defined pyrite, particles in the MgSi-only class were considered to be talc and those in the CaP-only class, apatite. Thirty-five classes of these: (i) "mineral type," (ii) other crustal type, and (iii) metal-bearing particles were identified, with the 36^{th} class for all particles remaining unclassifed. The metals Cr, Ni, Cu, Zn, As, Sb, and Pb were recorded over a range of concentrations in the individual particles and four metal-bearing particles classes were defined.

The CCSEM particle data for each sample was linearly sorted through the 36 class scheme, however for ease of comparison, class assignment outcomes were concatenated into "groups" of classes. Six "soil particle" class groups were delineated (Si-rich, AlSi, Fe-rich, Ca-rich, AlSiK, AlSiCa), one "metals" group reflecting metal-bearing particles and one "Pb-bearing" particle

301 group were specified, as well as a group referred to as “others” and those particles left
302 unclassified. The results of the group assignments, in terms of particle number attribution, for
303 each of the samples are set out in Figure 2.
304
305 The four samples that were collected as topsoil (RM71, RM72, BM5, and RM45)
306 characteristically recorded a high percentage of particles in the ‘soil particle’ groups. The AlSiK-
307 bearing particle group is important in all the soil samples. In the sample of RM77 the metals group
308 (Zn being important) dominates, and given that the RM77 sample was collected from the Gornje
309 Polje site, which was a repository for waste from the Zvecan smelter, this is not surprising. The
310 RM66 particle assemblage is dominated by Fe-rich, and Pb-bearing particles. Considering the
311 origin of this sample (Zarkov Potok tailings) we consider the Fe-rich and Pb-bearing particles that
312 populate this medium are of anthropogenic origin. Corresponding to the total Pb concentration
313 documented in the soils (Table 1), the abundance of Pb-bearing particles followed the order
314 BM5>RM71>RM72>RM45. Moreover, among all the samples, the highest percentage of the total
315 particles analyzed that contained Pb was recorded in sample BM5. As was to be expected, Pb was
316 identified frequently at the IP level in the samples, but was not observed in a mineral form. X-ray
317 Powder Diffraction (XRD) identified several (some uncommon) Pb-minerals in the Mitrovica
318 samples (Boisa et al., 2013). The XRD analysis of a tailing sample identified the minerals lanarkite
319 ($Pb_2(SO_4)O$), and beudantite ($PbFe_3(OH)_6SO_4AsO_4$); of an IDP camp soil the mineral coronadite
320 ($PbMn^{4+}{}_2Mn^{2+}{}_6O_{16}$); and of a smelter waste sample the minerals beudantite, coronadite,
321 cerussite ($PbCO_3$), and Anglesite ($PbSO_4$). However CCSEM analysis and visual inspection found

322 that the Pb was bound, at the IP level, with variety of other elements in many different physical
323 forms.
324
325 The particles initially assigned to the Pb-bearing particle class were subject to a separate
326 clustering exercise. A classification scheme for the Pb-bearing particles was created from the
327 CCSEM data using the same form of supervised divisive hierarchical cluster analysis. A 55 Pb-
328 particle classification scheme was created. Sifting the Pb-particle data from each sample data-set
329 through the 55-class scheme allowed the specificity of each class to be maximized. In the
330 resulting classification, seven of the Pb-particle classes were found to have minimal
331 discriminating power with less than 3% total for all sample particles reporting in any of these
332 classes. Consequently, a classification scheme containing 48 classes was used for Pb-particle
333 differentiation. The information in the 48 classes was later aggregated into 19 groups of similar
334 classes. The results obtained from the linear sorting of the Pb-particle data from each sample
335 through this scheme are set out in Table 2 (only percentage abundances > 1.0% are reported).
336 The class assignment of Pb-particles in each sample was largely restricted to a specific set of
337 classes, and for each sample these were different classes. Included in Table 2 is a list of elements
338 for each group which are the “defining” elements for the classes in that group. These are not the
339 only elements found in the particles assigned to classes for a specific group, they are, however,
340 the elements that are characteristic of these particles. For example, in Group 3 classes, with Fe
341 the other common element is Cu in the presence or absence of Ni (for illustrative purposes see
342 Figure 3c). Other elements may be present (e.g., Si and Zn in Figure 3c), but may be absent so do
343 not define the particles in these classes. The major group assignments for the percentage of Pb

344 particles in each sample were as follows: RM77: 90.6% to groups 1 and 2; RM66: 60.1% to groups
345 3 and 4; RM72: 52.93% to groups 5-7; BM5: 48.3% to groups 8-11; RM71: 45.9% to groups 12-15;
346 and, RM45: 64.7% to groups 16-19. These percentage assignments were highly specific for these
347 "signature" groups; these groups are monotypic in that they are characterized by a unique
348 representative particle type. For no sample were <46% of the sample particles assigned to the
349 sample signature groups. The signature groups (e.g., groups 1 and 2 for sample RM77) as ordered
350 in Table 2 form part of a source signature matrix (see e.g., Hunt et al., 1991) which could be used
351 for source attribution of Pb-particles in local samples of unknown origin (see Hunt et al., 1993).
352 However, the goal here was to demonstrate whether the Pb-particles in each sample were
353 distinctly different from those in the others. The results presented in Table 2 strongly
354 demonstrate this. The classification overlap (the percentage of Pb-particles from other samples
355 assigned to the signature groups of any specific sample), was relatively minor with a cross-
356 assignment of generally <4% and for no signature group was it >10%. Overlap between classes,
357 while small, was most obvious for the classes that characterized the Pb-bearing particles in the
358 soils, thus some windblown soil cross contamination might have existed.
359
360 The element characteristics of the Pb-particles, as reported by the signature groups,
361 appear to be the principal control on the Pb solubility in each sample. For example we
362 hypothesize, that for sample RM77 (with a UBM of 3%), Fe and Zn are the dominant elements
363 controlling the Pb solubility. For RM72 (UBM 13%), the presence of Ca and P conferred a lower
364 solubility of Pb, and, for the sample with the highest Pb bioaccessiblity (RM 45; UBM 89%), the

365 dominance of Si, Al, Fe, Mn (+/-As) with low levels of Pb in the Pb-particles resulted in high Pb
366 solubility
367
368 Operator inspection of Pb-bearing particles in the SEM from each sample confirmed the
369 CCSEM classification that there were a wide variety of Pb-particle forms in these samples. Specific
370 examples of Pb-particles, that match specific CCSEM classed particles, are set out in Figure 3.
371 Figure 3a is an example of the dominant particle type in RM77 where the uniform backscatter
372 contrast matrix contains Pb, Fe and Zn, while the particle in Figure 3b has a similar composition
373 but is an example of a particle that also contains As. Examples of sample RM66 Pb-particles that
374 would be assigned to classes in Group 3 (Ni- and Cu-bearing), and Group 4 (Fe- and Mn-bearing)
375 are set out in the images in Figure 3c and 3d respectively. Figure 3e is of a mixed phase particle
376 from RM72 that contains Ca and P that would be assigned to a Group 5 class, and the image in
377 Figure 3f, also of an RM72 Pb-particle, would be classified similarly although the Ca and P content
378 was much less. The examples of BM5 Pb-particles would be classed as Group 8 (Figure 3g) or
379 Group 11 (Figure 3h) particles. RM71 Pb-particles with very mixed composition (consisting of e.g.,
380 Al, Si, K, Fe, and Mn) are illustrated in Figure 3i and 3j. Lastly, examples of RM45 particles
381 dominated by Pb and Pb + Mn are set out in Figure 3k and 3L. Interestingly, none of the observed
382 Pb-particles resembled Pb-bearing paint particles, that contain Pb-pigment particles and other
383 particle types in an organic vehicle (see e.g., Hunt, 2016).
384
385 **Differential Individual Particle Analysis (DIPA)**

386 The recorded *in vitro* oral Pb bioaccessibilities of each of the samples in this study were
387 different and this is likely a function of how the Pb is bound in each. The CCSEM analysis and
388 individual Pb-particle imaging showed that the Pb in these samples was present in different
389 particle forms. It is our contention that this variability at the IP level controls Pb bioaccessibility.
390 To explore this notion, the Pb bioaccessibility associated with the various types of individual Pb-
391 particles in these samples was evaluated by DIPA. A detailed discussion of this analysis is beyond
392 the scope of this paper (Hunt and Entwistle, unpublished data), however here we present
393 examples of DIPA analysis of particles from each sample that we consider to be representative of
394 CCSEM signature group Pb-particles. It should be noted that bulk sample bioaccessibilty by UBM
395 used a sample size fraction of < 250 µm, while DIPA investigated particles <64 µm in size. The
396 possibility exists that larger 64-250 µm particles incorporated in the UBMB might lead to some
397 differences between UBM and DIPA bioacccessibility reporting. However, unless the larger
398 particles were systematically different across the sample set compared to the smaller particles
399 we expect the trend in bioaccessibilty across the samples (ranging from 3% t0 89%) to remain
400 consistent.
401
402 The lowest bulk sample Pb bioaccessibility was exhibited by sample RM77 (UMB of 3%)
403 and images of a typical Pb-bearing particle from this sample before any immersion in the SGF,
404 and after up to four sequential immersions of 30 minutes (2 hours total) are set out in Figures 3a
405 and 4a respectively. At the IP level, Pb appeared to be present in two forms in these particles.
406 The small high backscatter electron (bright) features in Figure 3a had a high Pb content and these
407 were solubilized after immersion in the SGF (compare with Figure 4a). In comparison, the matrix

of these particles was not dissolved during SGF immersion. We suggest, the Fe + Zn matrix material in which Pb was present acted to protect the matrix Pb from mobilization (Figure 4a). It appears that these dominant Pb-bearing particles in sample RM77 exhibited low Pb bioaccessibility because, (i) Pb was bound in the protective Fe + Zn matrix of the particles and, (ii) where small high Pb-particles were present, and were "locked" in the interior of these particles, as opposed to being on the surface (where they were easily solubilized when exposed to the SGF), they were protected from exposure to the SGF.

Sample RM66 had the second lowest Pb bioaccessibility (UBM of 6%) and it is likely that, just as in the case of sample RM77, the Pb in particles in RM66 was bound as a particle matrix element and the particles were resistant to dissolution in the SGF. In the case of RM66 particles with a high Fe+Mn content and a low Pb content they were not readily solubilized in the SGF. This is illustrated by comparing the image in Figure 3d of a Pb-particle before any SGF immersion with the image in Figure 4d of the same particle recorded after four sequential immersions of 30 minutes in the SGF. After the SGF immersion the composition and the form of the particle remained unaltered. The association of Pb bound as part of the matrix with Fe+Mn in the RM66 particles appears to have conferred protection from dissolution during SGF immersion.

The Pb bioaccessibility for sample RM72 (UBM of 13%) was marginally greater than for RM77 and RM66. This suggested that there were Pb-particle phases in this sample that were soluble during SGF immersion, although most were not. An example of an insoluble Pb-particle present in RM72 prior to SGF immersion and after four sequential immersions of 30 minutes in

the SGF is set out in Figure 3e and 4c. This Ca+P composition characteristics of this (Signature Group) particle appears to be a factor in reducing the Pb solubility.

Sample BM5 has a higher Pb solubility (UBM of 30%) and also had a wide range of different Pb-bearing particle types. Reviewing the diversity of Pb-particle types in BM5 is beyond the scope of this discussion; however, an example of a particle type (assigned to CCSEM Signature Group 11) minimally altered by immersion in the SGF is presented in Figure 4d. Prior to immersion in the SGF (Figure 3h), this particle recorded an Fe+Pb composition, however after four sequential immersions of 30 minutes (Figure 4d), while Fe+Pb were still present the elements Al and Si also became prominent. The size and shape of the particle post immersion does not appear to have changed significantly, although surface cracks had opened and/or widened, and clearly some SGF dissolution has occurred for these other elements to become more prominent in the EDS analysis.

Samples RM71 and RM45 had the highest Pb bioaccessibilty percentages (UBM of 88% and 89%, respectively), and this was reflected in the DIPA analysis. The RM71 Signature Group 12 particle in Figure 3i, had lost almost all Pb content after only 30 minutes immersion in the SGF (Figure 4e). The complicated element composition of this type of particle (with Al and Si being the dominant element) does not appear to confer and protection against Pb mobilization by the SGF. Similarly, where the Pb is present as a separate phase as in the example of the RM45 (Signature Group 17 particle in Figure 3l), the Pb is readily mobilized by the SGF. This is apparent from what remains of the particle shown in Figure 3l after exposure to the SGF for only 30 minutes (Figure 4f), the high Pb content phase in this particle has been completely solubilized.

Lead isotope Ratios

The isotope ratios $^{206}Pb/^{204}Pb$, $^{207}Pb/^{204}Pb$, and $^{208}Pb/^{204}Pb$ for the study samples are listed in Table 3. Also listed in Table 3 are Pb-isotope ratios published in the literature for the Trepča mine at Stan Terg (Brown, 1962; Jankovic, 1978) which is approximately 6 miles from Mitrovica. The main ore minerals at the Trepča mine are: galena, sphalerite, arsenopyrite, pyrite and pyrrhotite (Kolodziejczyk et al., 2012). The mine has been a major producer of Pb; since the start of modern exploitation of the mine in 1930 until 1998 it is estimated that the mine produced 2,066,000 metric tons of Pb (Féraud et al., 2007). The similarities in the ratios for each sample suggest that the Pb in each sample was from the same original ore source. While the bioaccessible Pb percentage varied substantially between samples the Pb isotope ratios did not provide any obvious clues as to why.

DISCUSSION

It is well known that Pb speciation in soils is a major factor influencing Pb bioaccessibility (e.g. Cox et al., 2013; Reis et al., 2014; Smith et al., 2011). Here, CCSEM is used to provide a detailed description of the constituent Pb-particle phases present in several surface soil samples that were collected from a geographically small area in Mitrovica, northern Kosovo. Of immediate significance for these samples was that, despite their close proximity when collected, the bulk sample Pb-concentration and the Pb bioaccessibility varied appreciably; ranging approximately between 625 and 47,000 mg/kg and 3.33 and 89% respectively. These differences were mirrored at the individual Pb-bearing particle level. In terms of Pb-particle composition we have demonstrated that Pb-particles in each sample conformed to specific element association types. Homogenous groups of particles, based on similarities in composition, were represented as one or several individual classes. For example in sample RM77, Pb associated with Fe and Zn at the IP level conform to a monotypic assemblage. That is, an assemblage based on particles that are all of the same type (element content) and are generated by the same process, or are of the same origin, but differ slightly in element percentages. For each of the study samples the constituent Pb-bearing particles were present as a polytypic assemblage (composed of several monotypic assemblages) that was different for each sample. The constituent monotypic assemblages for each sample clearly shared a commonality, and the intra-sample differences between monotypic assemblages were far smaller than any inter-sample differences. Hence different polytypic assemblages are recognized for each sample. For example, emergent from the CCSEM analysis, the polytypic assemblage of Pb-particles in sample RM77, defined by

Signature Groups 1 and 2 (Table 2) account for (describe) >90 % of the Pb-particles in the sample, and, the percentage of Pb-bearing particles from any of the other samples similar to RM77 particles (as specified by the element composition for Signature Groups 1 and 2), is <3%.

The presence of different polytypic Pb-particle assemblages across the study samples suggests that there are fundamental differences in the types of Pb-bearing particles present in the samples. From the Pb-isotope ratio data we concluded that the original source of the Pb in the samples was the same ore body of the Trepča mine. However, the forms of the Pb in the study samples suggest that the Pb in these samples has been modified from its original processed ore form. It is our contention that various manufacturing/industrial/anthropogenic (MIA) processes are responsible for this and, there has been dispersion in the environment either during MIA processing or subsequently, possibly with post-deposition transformation and repartitioning of the Pb in surface soils.

Differences in Pb bioaccessibility between samples appears to be a function of the differences in polytypic Pb-particle assemblages. These in turn are likely to be the result of various MIA processes that produced different Pb-bearing particle types in the samples. The samples exhibiting the lowest bioaccessibility (i.e., RM77 and RM66: ≤6 %) consist of monotypic assemblages dominated by the Pb associated with Fe and Zn and other first row transition metals (RM77) and Pb associated with Mn and other first row transition metals (RM66). When Pb is not matrix bound (e.g., with Zn and Mn) or locked as a Pb-dominant phase in a larger insoluble particle, but is present as a Pb-dominant phase either isolated, or attached to another particle, it

508 is relatively more bioaccessible. The association of Pb with other metals apparently confers a
509 resistance to SGF solubility. Undoubtedly, the elements in the Pb-particles are not present in a
510 'natural' unmodified form, which could increase solubility; however a passivation layer may have
511 developed conferring some protection.
512
513 The Pb-isotope ratio data provided almost no discriminating information on which to
514 separate the study samples from each other. The Pb-isotope information, production data, and
515 proximity, links the Pb in the study samples to the Trepča mine. Our Pb-isotope data closely
516 matches that obtained by Brewer et al., (2016) from samples collected in the same vicinity as the
517 study samples here. The $^{208}Pb/^{206}Pb$ data is similar in both studies. The $^{206}Pb/^{207}Pb$ data from this
518 study were tightly clustered in the range 1.186-1.196, while the $^{206}Pb/^{207}Pb$ data presented by
519 Brewer et al., (2016) was less clustered. Across this range our $^{206}Pb/^{207}Pb$ data for the Zharkov
520 Potok (RM66), Gornje Polje (RM77), Roma Mahalla topsoil (RM45), and IDP camp surface soils
521 (RM71 and RM72) sites correspond closely to results from the same sites set out in Brewer et al.,
522 (2016). This published data, and the data presented here, differs from that obtained from
523 samples from the same locales that has been described by Prathumratana et al., (2008). In the
524 Prathumratana et al., (2008) study, the sample $^{206}Pb/^{207}Pb$ data were all lower (<1.176); it is
525 unclear why this might be. Brewer et al., (2016) argued that the Pb in the surface soils from the
526 IDP camps originated from the Gornje Polje waste site. Here we show that the Pb in the samples
527 from Gornje Polje and the IDP camps are quite different from each other. At the bulk sample
528 level, the Pb bioaccessibility in each sample is different, and at the IP level the composition and
529 the solubility of Pb-bearing particles in each of these samples is different. We suggest that the

original source of the Pb in our study samples is the Trepca mine. This is in agreement with Brewer et al., (2016) who assert that the local Zvecan smelter is the source, and it is the Trepca mine that supplied the Zvecan smelter. Also, it is likely that the Pb in our samples has been modified from its original form by manufacturing/industrial/anthropogenic (MIA) processes. These "secondary" processes/sources cannot be readily identified by stable Pb-isotope ratio source attribution.

CONCLUSIONS

There is a growing acceptance that for PHEs exposure estimates can be improved by understanding the bioaccessibility of ingested material in the gastro-intestinal tract. As bioaccessibility is controlled by the chemical or mineral form (speciation) of the Pb, the more we understand the contaminant phases present in the soil, particularly in samples where the contaminant of interest is in complex phases, rather than present as discrete mineral phases, the better able we are to utilise and apply the bioaccessibility data. CCSEM particle characterization has the potential to provide additional supporting evidence for application in human health risk assessment and risk management. This is a relatively rapid, robust, and powerful tool that is capable of determining how various sample components are associated at the microscopic particle level. Results from the Mitrovica samples indicate that the Pb-particle types in these samples vary in form (morphology/habit), composition (separate phases vs. homogenous composition), and amount of Pb present at the IP level. Across the suite of samples, Pb-particles with metal associations were less soluble in the acidic environment of the gastric phase than low Pb-bearing particle types where the Pb takes the form of a surface coating or a separate concentrated phase. The results underline the importance of specific phases in tightly sequestering Pb in soils. However, when the Pb has been repartitioned in the soil, for instance if it has been sorbed onto the surfaces of other soil phases (across a range of soil mineral phases), then the Pb is more bioaccessible.

CCSEM-EDS, especially when allied to DIPA, can provide detailed information on particulates in environmental media which can help support environmental interpretations based on chemical extraction data to better refine subsequent risk-based assessments. CCSEM potentially also has a role to play in source attribution as data at the IP level inherently provides more information than bulk sample data alone. Recognizing the sources of contributing particles to a medium is of value for primary prevention of exposure to Pb enabling the removal of sources of lead exposure.

Whilst one might use CCSEM to usefully quantify the abundance of various Pb-phases in a sample, and to indicate possible source areas of particulate input, the actual Pb concentrations in the bioaccessible phase are also of relevance in situations such as these in Mitrovica where high total Pb concentrations actually mean that even where samples are dominated with low solubility Pb phases bioaccessible concentrations can reach nearly 3,000 mg/kg Pb. As such we contend that CCSEM-based analyses should not be considered a replacement for bioaccessibility, but that it can augment the understanding of such determinations and reduces the rather 'black-box' approach that has doggedly hampered the wider community acceptance of the utility and value of bioaccessibility testing at contaminated sites. Finally, detailed information provided by CCSEM analysis pre- and post-intervention implementation also has the potential to support decision-makers to evaluate the progress of any Pb reduction programs.

ACKNOWLEDGEMENTS

The authors would like to thank Graham Bird (Bangor), Paul Brewer (Aberystwyth) and Mark Macklin (Lincoln) for access to the samples, the Department of Earth Science and Environmental Sciences at UT Arlington for hosting Jane Entwistle as a visiting scholar during part of this work, and Asish Basu (Arlington) for facilitating the lead isotope analyses. Support for N. Boisa was provided by Rivers State University of Science and Technology, Nigeria, as part of a PhD program of research.

582 **REFERENCES**

583

584 Aguiar, A., Eubig, P.A., and Schantz, S.L. (2010). Attention deficit/hyperactivity disorder: a focused
585 overview for children's environmental health researchers. *Environ. Health Perspec.*, **118:**1646-
586 1653.

587

588 Ault, A.P., Peters, T.M., Sawvel, E.J., Casuccio, G.S., Willis, R.D., Norris, G.A., and Grassian, V.H.
589 (2012). Single-particle SEM-EDX analysis of iron-containing coarse particulate matter in an urban
590 environment: sources and distribution of iron within Cleveland, Ohio. *Environ. Sci. Technol.*,
591 **46**(8):4331-4339.

592

593 Bacon, J.R., and Davidson, C.M. (2008). Is there a future for sequential chemical extraction?
594 *Analyst* **133**(1):25-46.

595

596 Boisa, N., Bird, G., Brewer, P.A., Dean, J.R., Entwistle, J.A., Kemp, S.J., Macklin, M.G. (2013).
597 Potentially harmful elements (PHEs) in scalp hair, soil and metallurgical wastes in Mitrovica,
598 Kosovo: The role of oral bioaccessibility and mineralogy in human PHE exposure. *Environ. Int.,*
599 **60**:56–70.

600

601 Boisa, N., Elom, N., Dean, J.R., Deary, M., Bird, G., Entwistle, J.A. (2014). Development and
602 application of an inhalation bioaccessibility method (IBM) for lead in the PM_{10} size fraction of soil.
603 *Environment Int., **70:**132–142.*

Brewer, P.A., Bird, G. and Macklin, M.G. (2016). Isotopic provenancing of Pb in Mitrovica, northern Kosovo: Source identification of chronic Pb enrichment in soils, house dust and scalp hair. *Applied Geochemistry,* **64**:164-175.

Brown, J.S. (1962). Ore Leads and Isotopes. *Econ. Geol*., **57**:673-720.

Budtz-Jørgensen, E., Bellinger, D., Lanphear, B., Grandjean, P., et al. (2013). An international pooled analysis for obtaining a benchmark dose for environmental lead exposure in children. *Risk Anal.*, **33**(3):450-461.

Cai, M., McBride, M.B. and Li, K. (2016). Bioaccessibility of Ba, Cu, Pb, and Zn in urban garden and orchard soils. *Environmental Pollution*, **208**:145-152.

Chandramouli, K., Steer, C. D., Ellis, M. and Emond, A. M. (2009). Effects of early childhood lead exposure on academic performance and behavior of school age children. *Arch. Dis. Child,* **94**:844-848.

Chen, A., Cai, B., Dietrich, K.N., Radcliffe, J., and Rogan, W.J. (2007). Lead exposure, IQ, and behavior in urban 5- to 7-year-olds: does lead affect behavior only by lowering IQ? *Pediatrics* **119**(3):e650-658.

625 Conner, T.L., Norris, G.A., Landis, M.S., and Williams, R.W. (2001). Individual particle analysis of
626 indoor, outdoor, and community samples from the 1998 Baltimore particulate matter study.
627 *Atmos. Environ*. **35**:3935–3946
628
629 Cox, S.F., Chelliah, M.C.M., McKinley, J.M., Palmer, S., Ofterdinger, U., Young, M.E., Cave, M., and
630 Wragg, J. (2013). The importance of solid-phase distribution on the oral bioaccessibility of Ni and
631 Cr in soils overlying Palaeogene basalt lavas. Northern Ireland: *Environ. Geochem. Health.,*
632 **35**(5):553-567.
633
634 Coz, E., Gomez-Moreno, F.J., Pujadas, M., Casuccio, G.S., Lersch, T.L., and Artınano, B. (2009).
635 Individual particle characteristics of North African dust under different long-range transport
636 scenarios. *Atmos. Env*., **43:**1850–1863.
637
638 Donner, E., Ryan, C.G. Howard, D.L., Zarcinas, B., Scheckele, K.G., McGrath, S.P., de Jonge, M.D.,
639 Paterson, D., Naidu, R., Lombi, E. (2012). A multi-technique investigation of copper and zinc
640 distribution, speciation and potential bioavailability in biosolids. *Environ. Pollut*., **166**:57–64.
641
642 Duzgoren-Aydin, N.S. and Weiss, A.L. (2008). Use and abuse of Pb-isotope fingerprinting
643 technique and GIS mapping data to assess lead in environmental studies. *Environ Geochem.*
644 *Health*, **30**(6):577-88.
645

646 Farmer, J.G., Broadway, A., Cave M. R., Wragg, J., Fordyce, F., Graham, M., Ngwenya, B.T., and
647 Bewley R.J.T. (2011). A lead isotopic study of the human bioaccessibility of lead in urban soils
648 from Glasgow, Scotland., *Sci. Tot. Env*., **409**(23):4958–4965.
649
650 Féraud, J., Gani, M., and Vjollca, M. (2007). Famous Mineral Localities: The Trepca Mine Stari Trg,
651 Kosovo. *Min. Record*, **38**:267-298.
652
653 Grandjean, P. (2010) Even low-dose lead exposure is hazardous. *Lancet,* **376**(9744):85-856.
654
655 Gulson, B. (2008) Stable lead isotopes in environmental health with emphasis on human
656 investigations. *Sci. Total Environ.,* **400**(1-3):75-92.
657
658 Hunt, A., Johnson, D.L. and Thornton, I. (1991). Descriptive Apportionment of Lead in House Dust
659 by Automated SEM. *Water Air Soil Pollut*., **55-58**:69-77.
660
661 Hunt, A., Johnson, D.L., Watt, J.M. and Thornton, I. (1992). Characterizing the Sources of Lead in
662 House Dust by Automated Scanning Electron Microscopy. *Environ. Sci. Technol*., **26**:1513-1523.
663
664 Hunt, A., Johnson, D.L. and Thornton, I. (1993). Apportioning the Sources of Lead in House Dusts
665 in the London Borough of Richmond. *Sci. Total. Environ.,* **138**:183-206
666

667 Hunt, A. and D.L. Johnson (1996). Characterizing the Outlines of Degraded Fine-Particles by
668 Fractal Dimension. *Scanning Microscopy*, **10**:69-83.
669
670 Hunt, A. and Johnson, D.L. (2010). Differential Individual Particle Analysis (DIPA): Applications in
671 Particulate Matter Speciation Research. *J. Env. Qual*, **40**:742-750.
672
673 Hunt, A. (2016). Relative bioaccessibility of Pb-based paint in soil. *Environ. Geochem. Health,*
674 **38**:1037-1050.
675
676 Hunt, A. and Entwistle, J.A. (unpublished data). The Application of Differential Individual Particle
677 Analysis (DIPA) in the Characterization of Site-Specific Lead-Particle Phases that control the Lead
678 Bio-solubility in Contaminated Soils.
679
680 Jakubowski, M. (2011). Low-level environmental lead exposure and intellectual impairment in
681 children-the current concepts of risk assessment. *Int. J. Occup. Med. Environ Health*, **24**(1):1-7
682
683 Jankovic, S. (1978). The Isotopic Composition of Lead in some Tertiary Lead-Zinc Deposits within
684 the Serbo-Macedonian Metallogenic Province. *Geoloski anali Balkanskoga poluostrva*, **42**:507-
685 525.
686
687 Johnson, D.L. and A. Hunt (1991). Speciation of Lead in Urban Soils by Computer Assisted
688 SEM/EDX Method Development and Early Results. In Lead in Paint, Soil, and Dust: Health Risks,

689 Exposure Studies, Control Measures, Measurement Methods, and Quality Assurance, Eds. M. E.
690 Beard, S. D. A. Iske, ASTM International.
691
692 Kennedy, S.K., Walker, W., and Forslund, B. (2002). Speciation and Characterization of Heavy
693 Metal Contaminated Soils Using Computer-Controlled Scanning Electron Microscopy. *Environ.*
694 *Forensics*, **3**:131-143.
695
696 Kolodziejczyk, J., Prešek, J., Qela, H., and Asllani, B. (2012). New Survey of Lead and Zinc Ore
697 Mineralization in the Republic of Kosovo. *Geol. Geophys. Env*. **38**(3):295-306.
698
699 Kumar, P., Hopke, P.K., Rajaa, S., Casuccio, G., Lersch, T.L., and West R.R. (2012). Characterization
700 and heterogeneity of coarse particles across an urban area. *Atmos. Env*, **46**:449-459.
701
702 Lagudu, U.R.K., Raja, S., Hopke, P.K., Chalupa, D.C., Utell, M.J., Casuccio, G., Lersch, T.L., and West,
703 R.R. (2011). Heterogeneity of Coarse Particles in an Urban Area. *Environ. Sci. Technol.,*
704 **45**(8):3288–3296.
705
706 Lanphear, B.P., Hornung, R., Khoury, J et al. (2005). Low-level environmental lead exposure and
707 children's intellectual function: an international pooled analysis. *Environ. Health Perspec.*,
708 **113:**894-899.
709

710 Li, H-B., Li, K., Li, J., Ren, J-H., Luo, J., Juhasz, A. L., Cui, X-Y., Ma, L.Q. (2014). Assessment of in vitro
711 lead bioaccessibility in house dust and its relationship to in vivo lead relative bioavailability. *Env*
712 *Sci Technol*., **48:**8548-8555.
713
714 Lorenzi, D., Entwistle, J., Cave, M.R., Wragg, J., and Dean, J.R., (2012). The application of an in
715 vitro gastrointestinal extraction to assess the oral bioaccessibility of polycyclic aromatic
716 hydrocarbons in soils from a former industrial site. *Analytica Chimica Acta*., **735**:54–61
717
718 Moffet, R.C., Desyaterik, Y., Hopkins, R.J., Tivanski, A.V., Gilles, M.K., Wang, Y., Shutthanandan,
719 V., Molina, L.T., Abraham, R.G., Johnson, K.S., Mugica, V., Molina, M.J., Laskin, A., and Prather,
720 K.A. (2008). Characterization of aerosols containing Zn, Pb, and Cl from an industrial region of
721 Mexico City. *Environ. Sci. Technol.,* **42**:7091–7097.
722
723 Nigg, J., and Nikolas, M. (2008). Attention-Deficit/Hyperactivity disorder. In: Child and Adolescent
724 Psychopathology (Beauchaine TP, Hinshaw SP, eds). Hoboken, NJ: John Wiley & Sons.
725
726 Nigg, J.T., Nikolas, M., Knottnerus, G., Cavanagh, K. and Friderici, K. (2010). Confirmation and
727 extension of association of blood lead with attention-deficit/hyperactivity disorder (ADHD) and
728 ADHD symptom domains at population-typical exposure levels. *J. Child Psychol. Psychiatry*,
729 **51**(1):58-65.
730

731 Okorie, A., Entwistle, J., and Dean, J. R. (2011). The application of in vitro gastrointestinal
732 extraction to assess oral bioaccessibility of potentially toxic elements from an urban recreational
733 site. *Applied Geochem*., **26(**5):789–796.
734
735 Palumbo-Roe, B., Wragg, J., Cave, M. R., and Wagner, D. (2013). Effect of weathering product
736 assemblages on Pb bioaccessibility in mine waste: Implications for risk management. *Environ. Sci.*
737 *Pollut. Res*., **20**(11):7699-7710.
738
739 Pelfrêne, A., Waterlot, C., Mazzuca, M., Nisse, C., Cuny, D., Richard, A., Denys, S., Heyman, C.,
740 Roussel, H., Bidara, G., and Douay, F. (2012). Bioaccessibility of trace elements as affected by soil
741 parameters in smelter-contaminated agricultural soils: A statistical modeling approach. *Environ.*
742 *Pollut*., **160**:130–138
743
744 Prathumratana, L., Kim, R., and Kim, K. W. (2008). Heavy Metal Contamination of the Mining and
745 Smelting District in Mitrovica, Kosovo. Proc. Int. Symp. Geoscience Resources and Environments
746 of Asian Terranes, 4th IGCP 516, and 5th APSEG; Bangkok, Thailand, pp 479-482.
747
748 Rabinowitz, M.B. (1995). Stable isotopes of lead for source identification. *J. Toxicol. Clin. Toxicol*.,
749 **33**(6):649-55.
750

751 Reid, E.A., Reid, J.S., Meier, M.M., Dunlap, M.R., Cliff, S.S., Broumas, A., Perry, K. and Maring H.
752 (2003). Characterization of African dust transported to Puerto Rico by individual particle and size
753 segregated bulk analysis. *J. Geophys. Res*. **108**(D19):8591.
754
755 Reis, A.P., Patinha, C., Wragg, J., Dias, A.C., Cave, M., Sousa, A.J., Costa, C., Cachada, A., Ferreira
756 da Silva, E., Rocha, F., and Duarte, A. (2014). Geochemistry, mineralogy, solid-phase fractionation
757 and oral bioaccessibility of lead in urban soils of Lisbon. *Environ. Geochem. Health.* **35**(5):867-
758 881.
759
760 Roussel, C.H., Waterlot, C., Pelfrêne, A., Pruvot, C., Mazzuca, M., and Douay, F. (2010). Pb and
761 Zn Oral Bioaccessibility of Urban Soils Contaminated in the Past by Atmospheric Emissions from
762 Two Lead and Zinc Smelters. *Arch. Env. Contam. Toxicol*., **58**(4):945–954.
763
764 Roy, A., Bellinger, D., Hu, H., Schwartz, J., Ettinger, A.S., Wright, R.O., Bouchard, M., Palaniappan,
765 K., and Balakrishnan, K. (2009). Lead exposure and behavior among young children in Chennai,
766 India. *Environ. Health Perspec.*, **117:**1607-1611.
767
768 Smith, E.,Kempson, I. M., Juhasz, A. L., Weber, J., Rofe, A.; Gancarz, D., Naidu, R., McLaren, R.
769 G., Grafe, M. (2011). In vivo-in vitro and XANES spectroscopy assessments of lead
770 bioavailability in contaminated periurban soils. *Environ. Sci. Technol.*, ***45***(14), 6145-6152.
771
772

U.S. Department of Health and Human Services Food and Drug Administration (USFDA) (2016) "Harmful and Potentially Harmful Constituents" in Tobacco Products as Used in Section 904(e) of the Federal Food, Drug, and Cosmetic Act. 81 FR 28974. 3pp. http://www.fda.gov/TobaccoProducts/GuidanceComplianceRegulatoryInformation/ucm241339.htm (accessed 12/1/2016)

USEPA, (2007). Estimation of relative bioavailability of lead in soil and soil-like materials using in vivo and in vitro methods. OSWER 9285.7-77. USEPA, Washington, D.C.

Walraven, N., Bakker, M., Van Os, B.J.H., Klaver, G.Th., Middelburg, J.J., Davies, G.R. (2015). Factors controlling the oral bioaccessibility of anthropogenic Pb in polluted soils. *Science of the Total Environment*, **506-507:**149-163.

Wagner, J. and Casuccio, G. (2014) Spectral imaging and passive sampling to investigate particle sources in urban desert region. *Environ. Sci. Process. Impacts*, **16**(7):1745-1753.

Wragg, J., and Cave, M.R. (2012). Assessment of a geochemical extraction procedure to determine the solid phase fractionation and bioaccessibility of potentially harmful elements in soils: A case study using the NIST 2710 reference soil. *Anal. Chim. Acta.,* **772**:43-54.

Wragg J, Cave M, Taylor H, Basta N, Brandon E, Casteel S, et al. (2009). Inter-laboratory trial of a unified bioaccessibility procedure. Chemical & Biological Hazard Programme Open Report (OR/07/027); [90 pp.].

796 Young, S.D., Zhang, H., Tye, A.M., Maxted, A., Thums, C., and Thornton, I. (2005). Characterizing
797 the availability of metals in contaminated soils: I. The solid phase—Sequential extraction and
798 isotopic dilution. *Soil Use Manage.* **21(**S2):450–458.

799

800

List of Tables and Figures

Figure 4 Scanning electron microscope images of Pb-particles after SGF immersions of various durations documented in pristine form in Figures: 3a. (a., after 120 minutes), 3d. (b., after 120 minutes), 3e. (c., after 120 minutes), 3h. (d., after 120 minutes), 3i. (e., after 30 minutes), and 3l. (f., after 30 minutes)

Table 1. Sample location information, sample Pb summary data, and CCSEM analysis breakdown

Sample ID (type)	Site location	Bulk sample Pb concentration (mg/kg) [n=3]	Bioaccessible sample Pb (%) [n=3]	Total number particles analyzed by CCSEM	Subset [n] of Pb-bearing particles analyzed by CCSEM
RM71 (topsoil)	IDP camp	3,210 ± 24.0	88	4,592	434
RM72 (topsoil)	IDP camp	2,140 ± 8.50	13	6,000	273
BM5 (topsoil)	Bosniak Mahalla	8,670 ± 183	30	5,399	1,715
RM45 (topsoil)	Roma Mahalla	624 ± 25.7	89	5,743	72
RM66 (tailings)	Zarkov Potok	1,510 ± 8.9	5.8	5,158	1,012
RM77 (smelter waste)	Gornje Polje	46,900 ± 120	3.3	5,975	1,538

Table 2. CCSEM Pb-particle group assignments. 'Signature Group' assignments for specific samples are in bold.

GROUP # (#classes)	Defining Element	Sample Site Codes (percentage Pb bioaccessibility)					
		RM77 (3%)	**RM66 (6%)**	**RM72 (13%)**	**BM5 (30%)**	**RM71 (88%)**	**RM45 (89%)**
1 (6)	**Fe, Zn** (+/-As, +/- Cu, +/-S)	***79.8***	2.9	2.6	2.7	1.1	
2 (1)	**High Pb** (Fe, Zn, S)	***10.8***		2.6	2.4	2.0	
3 (3)	**Fe** (Cu and/or Ni)	3.7	***29.9***		3.2		1.5
4 (4)	**Fe, Mn** (+/-As)	2.6	***30.3***	2.8	3.4	4.2	2.9
5 (5)	P, Ca (+/-Fe, +/-Na, +/-Si)			***33.7***	1.5	3.3	
6 (2)	Fe		5.0	***9.6***	5.1	2.2	
7 (2)	Fe, Al, Si, Ca, Na (+/-K, +/-Mg)		1.3	***9.6***	0.4	2.2	4.4
8 (1)	Si, Fe, Al, As			2.2	***6.4***	3.8	
9 (3)	Si, Al, Fe, K (+/-Mg, +/-Ca)		2.1		***11.6***	4.2	
10 (1)	Si, Fe, Al, Ca, K, Mg		2.7	1.3	***13.6***	2.0	4.1
11 (2)	Fe, Si, Al (+/- Mg)		1.9	2.6	***16.8***	9.3	9.3
12 (4)	Si, Al, Fe, Na, K (+/-As, +/-Mg, +/-Mn)		2.5	1.7	1.2	***13.7***	3.1
13 (4)	Si, Al, Fe, Na, K (+/-Mg +/-Ca)		1.0	2.5	8.0	***17.6***	3.6
14 (2)	Fe, Si, Al, Na		3.1	7.0	3.7	***8.9***	1.5
15 (1)	Fe, Si, Al		1.5		2.0	***5.8***	1.5
16 (3)	Si, Al, Fe, Mn (+/-As)		4.8	1.3	6.2	7.5	***36.8***
17 (1)	Ca, Si, Fe, Al			7.4	2.4	2	***5.9***
18 (1)	Pb > 85%			1.0			***8.8***
19 (2)	Si (+/-Al)		2.9	2.6	5.1	9.1	***13.2***

Table 3. Pb Isotope ratios for study samples

	Isotope Ratios					
Sample ID	**$^{206}Pb/^{204}Pb$**	**2σ**	**$^{207}Pb/^{204}Pb$**	**2σ**	**$^{208}Pb/^{204}Pb$**	**2σ**
RM72	18.681	0.019	15.722	0.015	39.142	0.048
RM71	18.675	0.021	15.711	0.020	38.930	0.054
RM45	18.632	0.011	15.647	0.008	38.755	0.026
BM5	18.647	0.007	15.591	0.010	38.668	0.029
RM66	18.680	0.022	15.618	0.022	38.704	0.060
RM77	18.639	0.038	15.675	0.045	38.833	0.114
Trepca mine*	18.830		15.76		39.26	
Trepca mine**	18.890		15.14		39.46	

*from Brown (1962) **Jancovic (1978)

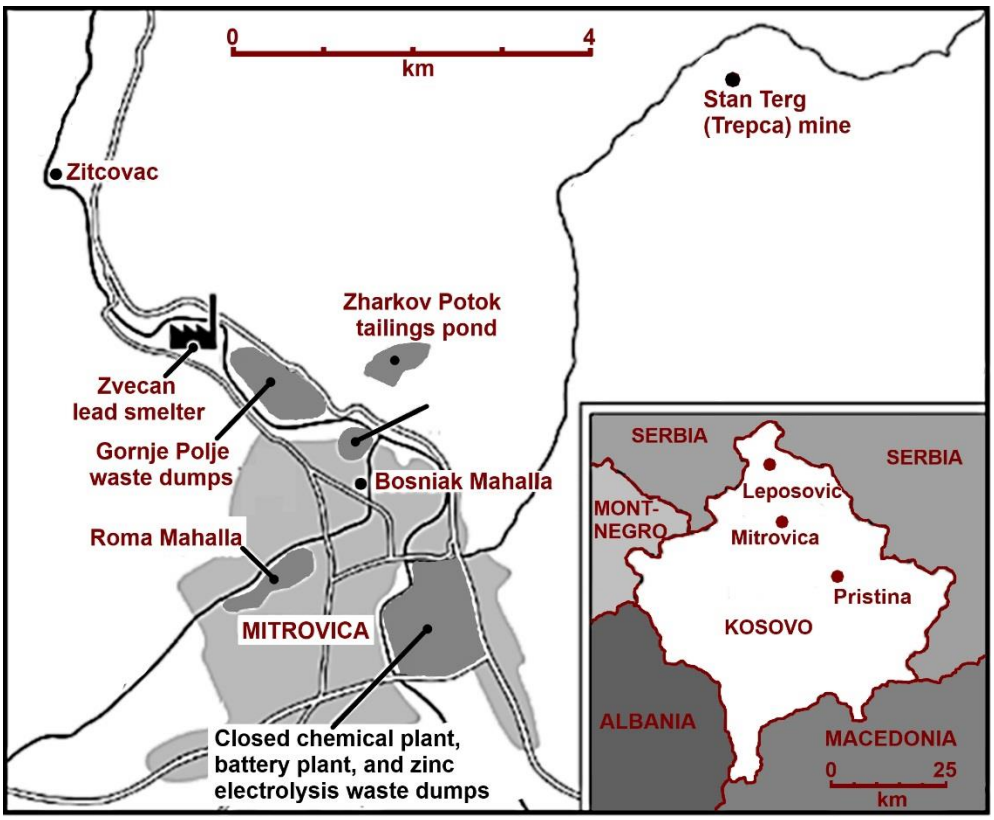

Figure 1 Study area showing the sampling locations, and locations of past metallurgical industries and the deposits of metallurgical waste (after Boisa et al., 2013).

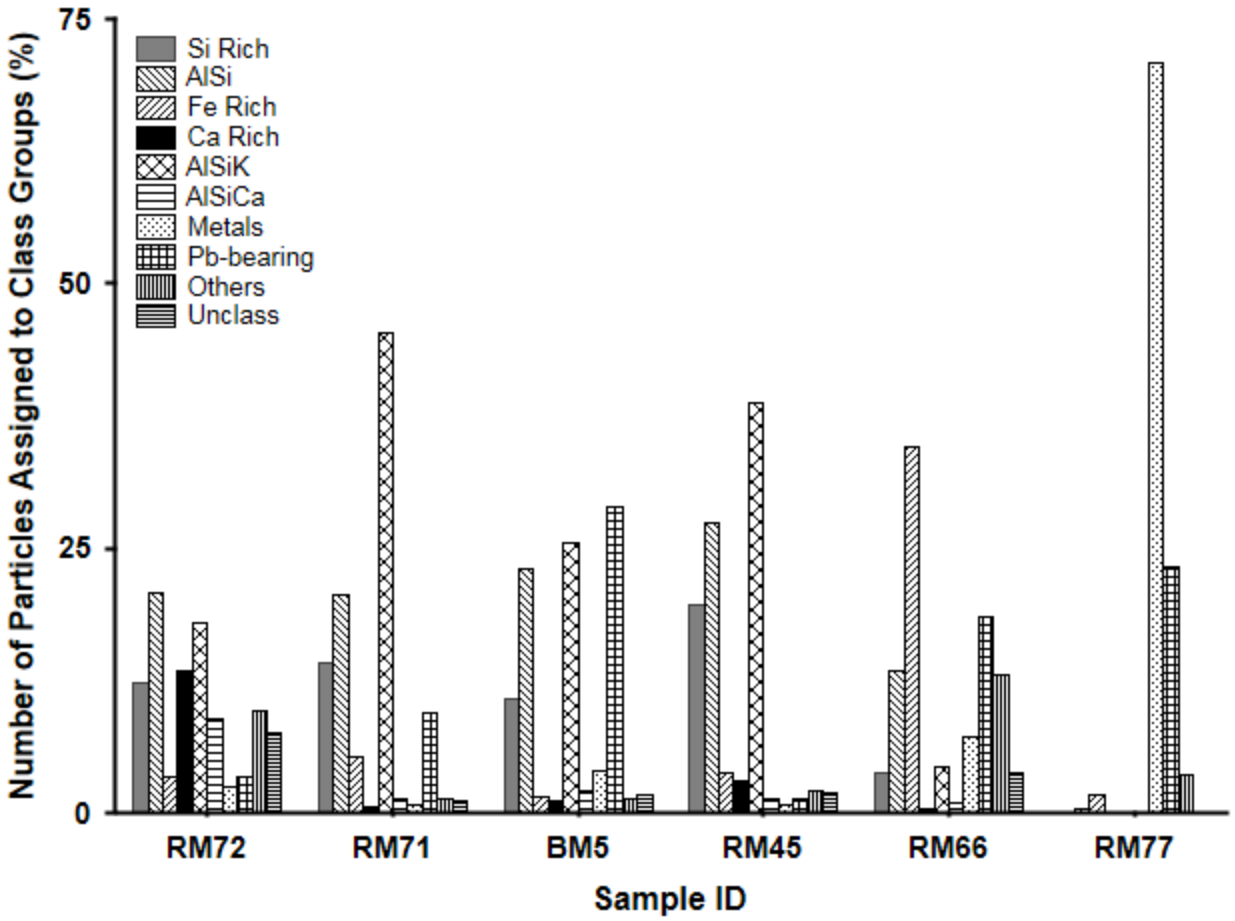

Figure 2 General classification of particles from the study samples using a consolidated version of the 58 class scheme developed for these samples

Figure 3

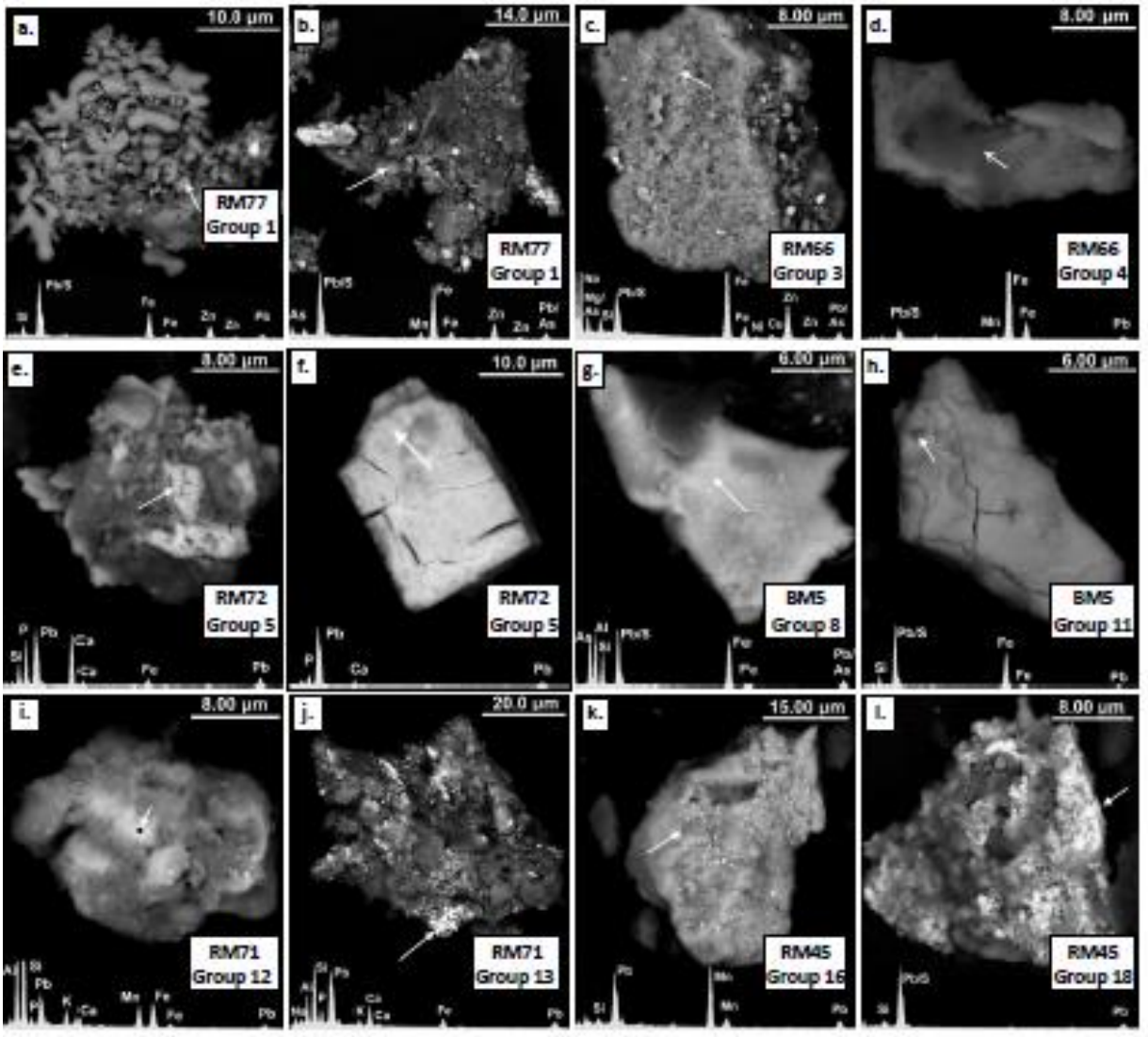

Figure 3 Scanning electron microscope images of pristine Pb-particles from each sample with compositions matching the classification scheme Groups: 1 (a., and b.) from sample RM77 total Pb-bioaccessibility: 3%; 3 (c.), 4 (d.) from sample RM66 total Pb-bioaccessibility: 6%; 5 (e., and f.) from sample RM72 total Pb-bioaccessibility: 13%; 8 (g.), 11 (h.) from sample BM5 total Pb-bioaccessibility: 30%; 12 (i.), 13 (j.) from sample RM71 total Pb-bioaccessibility: 88%; and 16 (k.), and 18 (l.) from sample RM45 total Pb-bioaccessibility: 89%

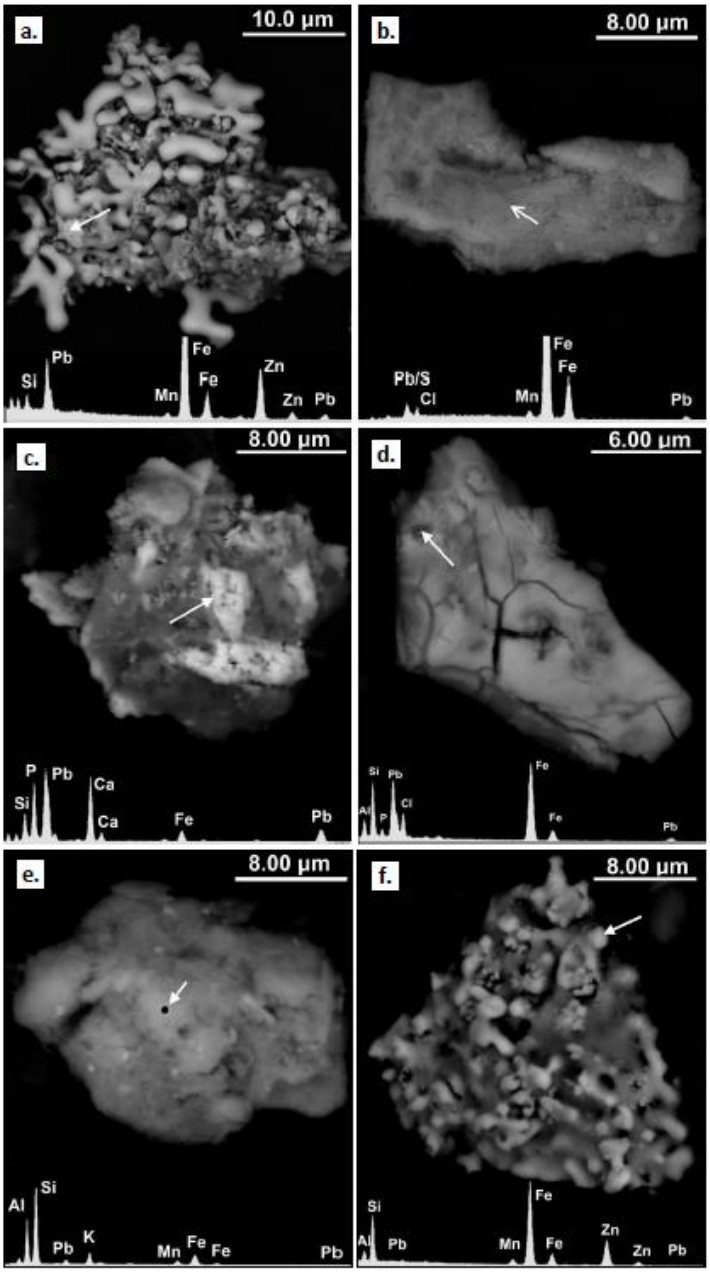

Figure 4 Scanning electron microscope images of Pb-particles after SGF immersions of various durations documented in pristine form in Figures: 3a. (a., after 120 minutes), 3d. (b., after 120 minutes), 3e. (c., after 120 minutes), 3h. (d., after 120 minutes), 3i. (e., after 30 minutes), and 3l. (f., after 30 minutes)